Journal of Applied Polymer Science

Antifouling and Blood-Compatible Poly(ether sulfone) Membranes Modified by Zwitterionic Copolymers via *In Situ* Crosslinked Copolymerization

Jing-Jing Wang,[1] Ming-Bang Wu,[1] Tao Xiang,[1] Rui Wang,[1] Shu-Dong Sun,[1] Chang-Sheng Zhao[1,2]

[1]College of Polymer Science and Engineering, State Key Laboratory of Polymer Materials Engineering, Sichuan University, Chengdu 610065, People's Republic of China

[2]National Engineering Research Center for Biomaterials, Sichuan University, Chengdu 610064, People's Republic of China

J.-J. Wang and M.-B. Wang contributed equally to this work.

Correspondence to: T. Xiang (E-mail: xita198906@163.com) and C.-S. Zhao (E-mail: zhaochsh70@163.com)

ABSTRACT: A novel and simple but practical method for the preparation of modified poly(ether sulfone) (PES) membranes was provided by the *in situ* crosslinked copolymerization of sulfobetaine methacrylate (SBMA) and sodium *p*-styrene sulfonate (NaSS) in PES solution followed by a phase-separation technique. Then, semi-interpenetrating network membranes modified by the crosslinked copolymers of poly(sulfobetaine methacrylate-*co*-sodium *p*-styrene sulfonate) [P(SBMA-*co*-NaSS)] were prepared. The SBMA-containing copolymer-modified membranes showed improved protein antifouling properties with flux recovery ratios above 90%. Furthermore, the anticoagulant properties of the NaSS-containing copolymer-modified membranes were obviously enhanced; their activated partial thromboplastin time could be prolonged to about 115 s. Thus, the P(SBMA-*co*-NaSS) zwitterionic copolymer-modified membranes showed improved antifouling properties and blood compatibility and will provide wide choices for their specific applications. © 2014 Wiley Periodicals, Inc. J. Appl. Polym. Sci. **2015**, *132*, 41585.

KEYWORDS: adsorption; biocompatibility; copolymers; crosslinking; membranes

Received 7 June 2014; accepted 1 October 2014

DOI: 10.1002/app.41585

INTRODUCTION

Artificial materials have been widely applied in biomedical fields, such as in artificial organs, disposable clinical instruments, and hemodialysis devices.[1,2] Excellent biocompatibility is essential and necessary for artificial materials, and blood compatibility has been considered to be the most important part of biocompatibility.[3] When in contact with blood, the nonspecific adsorption of proteins such as fibrinogen and clotting enzymes on biomaterial surfaces is recognized as the first interaction event of many undesired bioreactions and bioresponses; it is followed by platelet adhesion, activation of coagulation pathways, and thrombus formation.[4,5] Among these artificial materials, poly(ether sulfone) (PES) has been widely applied in the fields of artificial organs and medical devices used for blood purification[6] for its good thermal and chemical stabilities and good mechanical properties.[7,8] However, when pristine PES membranes were used as the blood-contact material, their biocompatibility was not adequate. Thus, it is necessary to modify PES membranes to endow them with improved antifouling properties and blood compatibility.

Recently, zwitterionic polymers have attracted much attention in the biomedical field because they can improve the antifouling properties and blood compatibility of materials.[9,10] It is believed that these materials surfaces (either zwitterionic groups or a mixture of anionic and cationic terminal groups) are resistant to nonspecific protein adsorption; this was realized by a hydration layer bound through the solvate of the charged groups in addition to hydrogen bonding.[11] As is known, water molecules form strong hydrogen bonding easily. Materials can interact and combine water molecules by hydrogen bonding near the surface, and then, a hydration layer is formed, which will act as a physical and energetic barrier to prevent protein adsorption on the surface.[12] It has been reported that the nonspecific adsorption of proteins such as fibrinogen and clotting enzymes on biomaterial surfaces is recognized as the first interaction event of many undesired bioreactions and bioresponses; it is followed by platelet adhesion and the activation of coagulation pathways,

Additional Supporting Information may be found in the online version of this article.

Table I. Compositions of the Copolymerization of SBMA and NaSS in PES Solutions

Sample	PES (wt %)	SBMA (wt %)	NaSS (wt %)	SBMA/NaSS molar ratio	MBA (mol %)[a]	AIBN (mol %)[a]
M-0	16	—	—	—	—	—
M-1	16	6	0	1:0	2	2
M-2	16	4	1.47	1:0.5	2	2
M-3	16	3	2.21	1:1	2	2
M-4	16	2	2.95	1:2	2	2
M-5	16	0	4.43	0:1	2	2

[a] The molar percentage was with respect to the total moles of the monomers (21.5 mmol for the membranes).

which leads to thrombus formation. Although the antifouling properties of zwitterionic-polymer-modified membranes are significantly increased, the blood compatibility of the membranes should be improved.[5,13,14] Poly(sulfobetaine methacrylate) (PSBMA), with a methacrylate main chain and a pendant group of taurine betaine [$-CH_2CH_2N^+(CH_3)_2CH_2CH_2CH_2SO_3^-$], is one of the most widely studied zwitterionic polymers.[12,15] Both experimental and theoretical studies have suggested that the antifouling properties of zwitterionic betaines stem from the opposite charges being highly hydrated.[12,16] In our previous studies,[15,17] PSBMA was used to modify the polysulfone (PSf) membrane by the surface-initiated atom transfer radical polymerization and click-chemistry-enabled layer-by-layer assembly. The modified membranes exhibited excellent antifouling properties and showed resistance to protein adsorption and platelet adhesion. However, the anticoagulant properties of the modified membranes were hardly improved. In some cases, the anticoagulant properties were of great importance for blood-contact medical devices, such as hemodialysis membranes and plasma fractionation membranes.[18–21] Thus, excellent blood compatibility and especially anticoagulant properties are important.

It is well known that heparin is widely used as an anticoagulant reagent, and its anticoagulant ability has mainly been attributed to the sulfonic groups and carboxyl groups in heparin, which can bind coagulation factors.[22,23] In recent years, sulfonic groups have been investigated extensively to prepare heparin-like polymeric materials with improved anticoagulant properties.[22,24] These reports have noted that sulfonated polymers showed good anticoagulant activity because the negatively charged pendent sodium sulfonic ($-SO_3Na$) groups expelled blood components by electrical repulsion because platelets, red blood cells, and plasma proteins in the blood showed electronegativity. The proteins existing on the outsides of these components, such as platelets and red blood cells, showed electronegativity because of ionization *in vivo,* for which the pH was about 7.4. Platelets, red blood cells, and other components in the blood showed electronegativity because of the cationic proteins.[18,25] Thus, these sulfonated-polymer-modified materials reduced nonspecific adsorption and platelet adhesion and then improved anticoagulant activity.[24,26] Many methods have been used to modify membranes, including the coating method, blending method, grafting method, and controlled living radical copolymerization.[27–31] In recent years, *in situ* polymerization, as a special blending technique, has been used to improve the compatibility of components in the polymer.[32,33] In our recent study,[34] a crosslinking agent was used in a synthesis process to obtain a stable semi-interpenetrating network (semi-IPN) structure. An *in situ* crosslinked free-radical polymerization/copolymerization was applied to modify commodity polymers, such as PES, PSf, poly(vinylidene fluoride), and polystyrene, to endow them with stimuli-responsive, antifouling, antibacterial, and blood-compatible properties.

In this study, zwitterionic copolymers of poly(sulfobetaine methacrylate-*co*-sodium *p*-styrene sulfonate) [P(SBMA-*co*-NaSS)] were synthesized by *in situ* crosslinked copolymerization in PES solutions. The solution was then used directly to prepare ultrafiltration (UF) membranes by a phase-separation technique. The permeability properties, antifouling properties, and blood compatibility for different copolymer-modified membranes were systematically investigated.

EXPERIMENTAL

Materials

PES (Ultrason E6020P) was purchased from BASF. Sulfobetaine methacrylate (SBMA) was synthesized according to the procedures described by Lowe and McCormick.[35] Sodium *p*-styrene sulfonate (NaSS; 90%, Aladdin), 2,2′-azobis(2-methylproronitrile) (AIBN; 99%, Aladdin), *N*,*N*′-methylene bisacrylamide (MBA; 99%, Aladdin), dimethyl sulfoxide (DMSO; 99.8%, Aladdin), sodium dodecyl sulfate (SDS; 92.5%, Aladdin), and sodium chloride (NaCl; 99%, Kelong) were used as received. Bovine serum albumin (BSA; fraction $V \geq 95\%$) and bovine serum fibrinogen (BFG; $\geq 75\%$) were obtained from Sigma Chemical Co. Micro BCA protein assay reagent kits were obtained from Pierce. The activated partial thromboplastin time (APTT) and thrombin time (TT) reagent kits were purchased from Siemens. Deionized water was used throughout the study.

Preparation of Modified Membranes with Semi-IPN Structures

Zwitterionic copolymers of P(SBMA-*co*-NaSS) with different chemical compositions were synthesized in PES solutions via the *in situ* crosslinked copolymerization of SBMA and NaSS, as shown in Table I. The synthesis procedure was as follows: PES was first dissolved in DMSO under stirring to get a homogeneous solution. Then, the reagents SBMA, NaSS, MBA, and AIBN dissolved in DMSO were added to the PES solution. The

polymerization was carried out at 75°C with vigorous stirring at 400 rpm for 24 h under nitrogen atmosphere.

After being cooled to room temperature and vacuum degassing, the polymerization solutions were directly prepared into membranes by spin coating coupled with a liquid–liquid phase-separation technique at room temperature. The prepared membranes were rinsed with deionized water thoroughly to remove the residual solvent.

Characterization

Fourier transform infrared (FTIR) spectra were obtained by a Nicolet 560 instrument (Nicolet Co.). To prepare the FTIR samples, the membranes were dissolved in DMSO and cast onto a potassium bromide (KBr) disc with a thickness of about 0.8 mm, and then, the casting solution was dried by an IR light.

Thermogravimetric analysis was obtained from a TG209F1 TG instrument (Netzsch, Germany) at a heating rate of 10°C/min under an N_2 atmosphere. The membranes were dried at 60°C to remove moisture before the measurement.

The composition of the membranes was determined by ^{1}H-NMR spectroscopy in DMSO-*d* with a Varian Unity Plus 300/54 NMR spectrometer. The characteristic aromatic peaks of the PES and the peaks of SBMA and NaSS were used to determine the composition.

Elemental analysis based on the determination of carbon (C), sulfur (S), hydrogen (H), and nitrogen (N) was performed by means of a Carlo Erba 1106 elemental analyzer (Italy) with a carrier gas (He, at a flow rate of 100 mL/min) at a combustion temperature of 1000°C with the solid samples. The proportions of C, S, H, and N for M-1, M-3, and M-5 were determined, respectively.

The morphologies (surfaces and cross sections) of the membranes were observed by scanning electron microscopy (SEM; JSM-5900LV, JEOL, Japan) with a voltage of 5 kV. The membrane samples were dried overnight in a vacuum oven at room temperature, then quenched by liquid nitrogenous gas, attached to the sample supports, and coated with a gold layer. The surface chemical compositions were confirmed by attenuated total reflection (ATR)–FTIR spectra, which were collected at a resolution of 4 cm^{-1}, and the reflectance spectra were scanned over the range 675–4000 cm^{-1}.

The hydrophilicity of the membrane surface was characterized by water contact angle (WCA) measurement with a contact angle goniometer (OCA20, Dataphysics, Germany) equipped with video capture at room temperature. One drop of water (3 μL) was dropped onto the surface of the membrane with an automatic piston syringe and photographed. The contact angles were measured continuously for 200 s for each sample. The contact angles data were determined from these images with a circle-fitting algorithm.

UF Experiments

The flux of the membrane was measured with an apparatus described in our previous procedure.[36] A dead-end UF cell with an effective area of 3.8 cm^2 was used, and the pressure was supplied by an air compressor. The test membrane was precompacted by deionized water for 30 min at a pressure of 0.08 MPa to obtain steady filtration. Then, the flux was measured at a pressure of 0.04 MPa. The pressure influenced the UF experiments, especially the UF of the BSA solution. On the basis of similar measurements from our previous studies,[36,37] a pressure of 0.04 MPa was chosen. All of the flux measurements were conducted at room temperature.

UF of Pure Water. The pure water flux values of the membranes were determined by the collection of the solution after it was steady. The flux of pure water was calculated by the following equation:

$$\text{Flux} = \frac{V}{Spt} \tag{1}$$

where V is the volume of the permeated solution (mL), S is the effective membrane area (m^2), P is the pressure applied to the membrane (mmHg), and t is the time for collecting the solution (h).

UF of the BSA Solution. As for the UF of the BSA solution, BSA was dissolved in an isotonic phosphate-buffered saline solution (PBS; pH 7.4) with a concentration of 1.0 mg/mL. The flux of the BSA solution was calculated by eq. (1). The BSA rejection ratio (R) was defined as follows:

$$R = \left(1 - \frac{C_p}{C_f}\right) \times 100\% \tag{2}$$

where C_p and C_f are the BSA concentrations of the permeate and feed solutions (mg/mL), respectively. The BSA concentration was measured by an ultraviolet–visible spectrophotometer (UV-1750, Shimadzu, Japan) at a wavelength of 278 nm.

To evaluate the antifouling properties of the membranes, PBS and BSA solutions were alternately applied to the membranes. The antifouling properties were expressed as the flux recovery ratio (F_{RR}), which was calculated by the following equation:

$$F_{RR} = \frac{F_2}{F_1} \times 100\% \tag{3}$$

where F_1 and F_2 are the PBS solution fluxes before and after the protein solution UF (mL $m^{-2}{\cdot}h^{-1}{\cdot}mmHg^{-1}$).

Blood Compatibility

Plasma Collection. Healthy human fresh blood (from a 28-year-old man) was collected with vacuum tubes (5 mL, Terumo Co.) containing a citrate/phosphate/dextrose/adenine-1 mixture solution (CPDA-1) as the anticoagulant (anticoagulant-to-blood ratio = 1:9). The blood was centrifuged at 1000 or 4000 rpm for 15 min to obtain platelet-rich plasma (PRP) or platelet-poor plasma (PPP), respectively.

All of the blood compatibility experiments were performed in compliance with relevant laws and institutional guidelines.

Protein Adsorption. Protein adsorption experiments were carried out with BSA and BFG solutions (PBS) with a concentration of 1 mg/mL. The membranes (1 × 1 cm^2) were first incubated in PBS for 24 h, equilibrated at 37°C for 2 h, and then immersed in BSA or BFG solution at 37°C for 2 h. After protein adsorption, the membranes were rinsed three times with PBS and deionized water separately to remove the loosely

Table II. Results of the Semiquantitative Analysis Based on FTIR Spectroscopy

Sample	Area of the peaks		a^*/b^* peak area ratio
	a^*	b^*	
M-0	0	0	—
M-1	121.702	54.314	2.241
M-2	70.219	32.782	2.142
M-3	43.898	25.618	1.713
M-4	21.461	17.643	1.216
M-5	0	21.667	0

a^*, peak of the ester groups ranging from 1700 to 1760 cm^{-1}; b^*, peak of the sulfonic groups ranging from 1025 to 1045 cm^{-1}.

bound protein from the membranes. Then, the membranes were immersed in a 2 wt % aqueous SDS solution at 37°C for 1 h under an agitation of 200 rpm to remove the protein adsorbed onto the membrane. The amount of protein eluted into the SDS solution was quantified by Micro BCA protein assay reagent kits, and the protein concentration was measured by an ultraviolet–visible spectrophotometer (UV-1750, Shimadzu, Japan) at a wavelength of 562 nm. More than 95% of the adsorbed protein were eluted into the SDS solution.

Platelet Adhesion. The membranes (1 × 1 cm^2) were incubated in PBS at 4°C for 24 h and equilibrated at 37°C for 1 h. After the PBS was removed, the membranes were incubated in 1 mL of fresh PRP at 37°C for 2 h. Then, the membranes were washed with PBS three times and treated with 2.5 wt % glutaraldehyde in PBS at 4°C for 1 day. Finally, the samples were washed with PBS and subjected to a drying process of graded alcohol–PBS solutions (25, 50, 70, 90, 95, and 100%) and isoamyl acetate–alcohol solutions (25, 50, 75, and 100%) for 15 min each time. The critical point during the drying of the samples was done with liquid CO_2. The number of adhering platelets on the membranes was calculated from five SEM pictures at 1000× magnification from different places on the same membrane. The numbers were finally averaged to obtain a reliable value.

APTT and TT. The antithrombogenicity of the membranes, including APTT and TT, was determined with an automated blood coagulation analyzer (CA-50, Sysmex Co., Japan). The APTT was measured as follows: the sample membranes (0.5 × 0.5 cm^2, four pieces) were immersed in PBS at 4°C for 24 h and equilibrated at 37°C for 1 h. Then, the PBS was removed, and 100 μL of fresh PPP was introduced. After incubation at 37°C for 30 min, 50 μL of the incubated PPP was added to a test cup; this was followed by the addition of 50 μL of APTT agent (which was incubated for 10 min before use). After incubation at 37°C for 3 min, 50 μL of a 25 m*M* $CaCl_2$ solution was added, and then, the APTT was measured. For TT, 100 μL of TT agent was added to the test cup (containing 50 μL of the incubated PPP), and then, the TT was measured.

RESULTS AND DISCUSSION

Characterization of the Membranes

The different solubilities of the membranes in DMSO verified the semi-IPN structure in the modified membranes. As shown in Figure S1 in the Supporting Information, the pristine PES membrane (M-0) was dissolved completely in DMSO. For M-1 and M-3, precipitation was observed clearly at the bottom of the tubes because of the cross-linked section in the membranes, which could swell in solvents.

FTIR spectra were used to characterize the bulk chemical compositions of the membranes; the data are shown in Figure S2 in the Supporting Information. As shown in the figure, for M-1 and M-3, new bands at 1725 and 1033 cm^{-1} were observed and compared with the spectra of M-0; they were attributed to the ester groups of PSBMA and sulfonic groups in the PSBMA and poly (sodiump-styrene sulfonate) (PNaSS), respectively. For M-5, only the band at 1033 cm^{-1} was observed. We also found that the integral of the band at 1725 cm^{-1} decreased with decreasing PSBMA content in the copolymer. In addition, the semiquantitative analysis based on FTIR spectroscopy was carried as shown in Table II; this reflected a tendency of variation to some extent. It showed that the peak area ratios were basically consistent with the theoretical results. The previous results demonstrated that the copolymers of P(SBMA-*co*-NaSS) were successfully synthesized in the PES solution.

The chemical compositions of the membrane surfaces were then confirmed by ATR–FTIR spectra, as shown in Figure 1. For the PSBMA and P(SBMA-*co*-NaSS) modified membranes (M-1∼M-4), a band at 1725 cm^{-1} was observed; this was attributed to the ester groups of PSBMA. The integrals decreased with decreasing PSBMA content in the membranes; this was consistent with the FTIR results of the membranes. The FTIR and ATR–FTIR results illustrate that the P(SBMA-*co*-NaSS) copolymers were successfully synthesized and incorporated into the PES membranes.

Thermogravimetric analysis, ^{1}H-NMR spectroscopy, and elemental analysis (Figures S3 and S4 and Table S1 and S2 in the Supporting Information) were used to define the quantitative

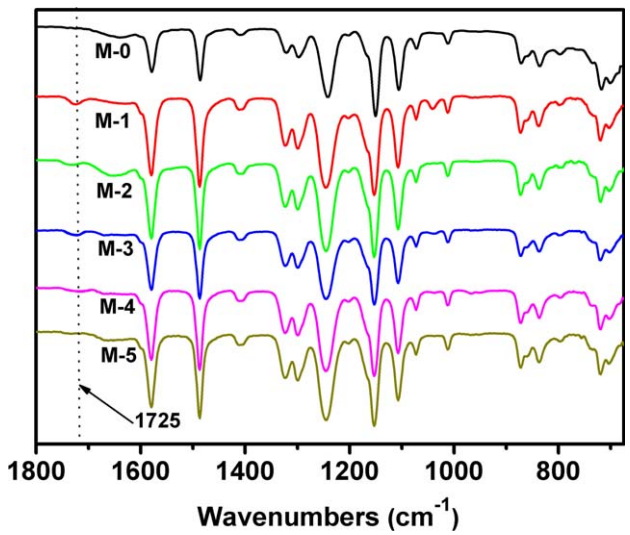

Figure 1. ATR–FTIR spectra for the pristine and modified PES membranes. [Color figure can be viewed in the online issue, which is available at wileyonlinelibrary.com.]

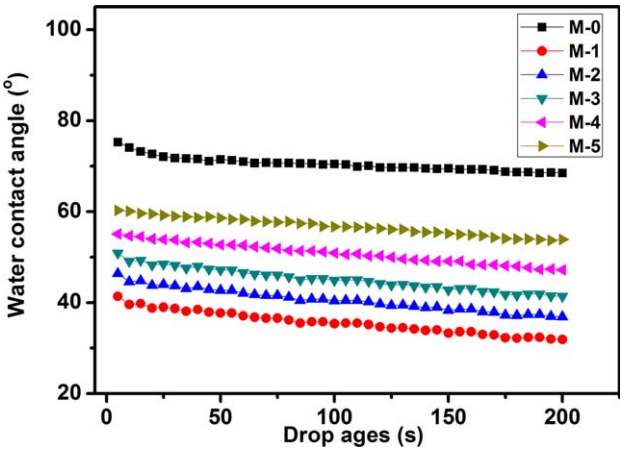

Figure 2. WCAs of the membranes. Values are expressed as the means plus or minus the standard deviation, $n = 3$. [Color figure can be viewed in the online issue, which is available at wileyonlinelibrary.com.]

interpenetrating amounts of zwitterionic copolymer, but these methods failed to accurately define the amounts. The details are shown in the Supporting Information.

WCA Analysis

WCA analysis is a convenient way to assess the hydrophilicity of the membrane surface, and it provides information on the interaction energy between the surface and the liquid.[38] The WCA measurements from 0 to 200 s for the membranes are shown in Figure 2. All of the modified membranes were more hydrophilic than the pristine PES membrane. For the modified membranes, we also found that the WCAs increased with decreasing SBMA in the copolymers; this indicated that SBMA contributed greatly to the increase in the membrane hydrophilicity. Meanwhile, the WCAs decreased with time for all of the membranes; this might have due to water evaporation because it is a measurement of the WCA in slow receding conditions.

Morphology of the Membranes

SEM was used to investigate the surfaces and cross sections of the membranes. Figure 3(a) shows the surface images of the membranes. We observed that the surface of M-0 was quite smooth. After the P(SBMA-*co*-NaSS) copolymers were introduced into the membranes (M-1∼M-5), some pores were observed on the surfaces. The reason might have been that the hydrophilic P(SBMA-*co*-NaSS) copolymers had an effect on the

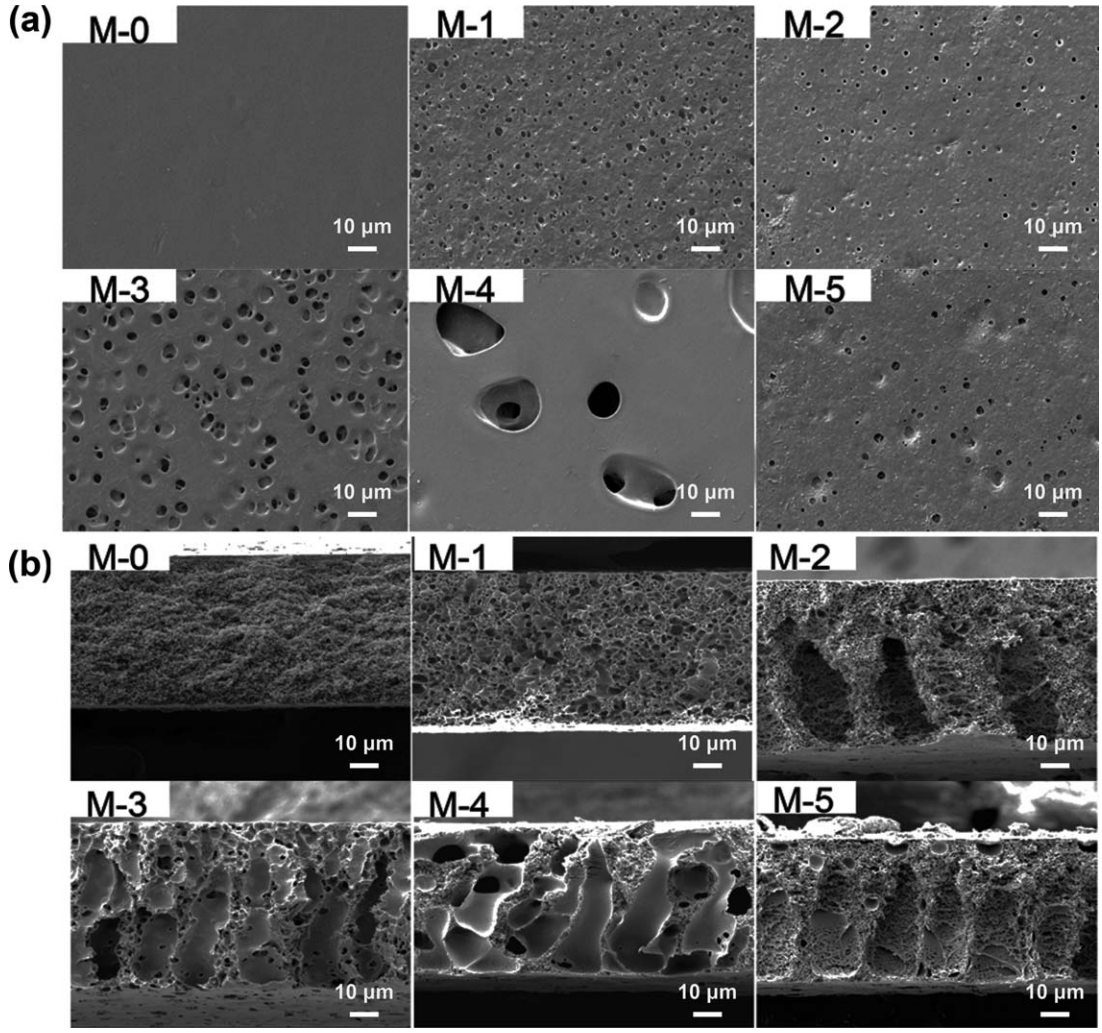

Figure 3. SEM images of the membranes: (a) surfaces and (b) cross sections.

Table III. Permeation Properties of the Pristine PES and P(SBMA-*co*-NaSS) Copolymer-Modified Membranes

Sample	Wall thickness (μm)	Pure water flux (mL m^{-2}·h^{-1}·$mmHg^{-1}$)	R (%)	F_{RR} of BSA UF (%)		
				First cycle	Second cycle	Third cycle
M-0	55 ± 3	808.12	34.32	68.21	70.81	74.50
M-1	55 ± 3	528.86	47.70	99.11	99.21	99.86
M-2	55 ± 3	120.10	88.73	70.67	95.00	97.19
M-3	55 ± 3	155.89	59.93	71.86	93.80	95.09
M-4	55 ± 3	210.98	50.21	80.14	96.50	99.84
M-5	55 ± 3	148.74	65.50	62.74	76.32	82.69

exchange between water and DMSO. The cross-sectional images are shown in Figure 3(b). As shown in the figure, for the membranes M-0 and M-1, a spongy structure was observed, and the structure was evenly distributed in the cross section except for the top and bottom layers. The images of the PES membrane (with DMSO as the solvent) were different from those of the PES membranes prepared with dimethylacetamide and *N*-methyl pyrrolidone as the solvents,[36,39] for which there was a skin layer, and followed a fingerlike structure. For membranes M-2 to M-5, large amounts of macrovoids were observed. The reason might have been that the hydrophilic P(SBMA-*co*-NaSS) copolymers had an effect on the liquid–liquid phase-separation process; this influenced the exchange between the DMSO solvent and water. What was interesting was that the M-4 membrane surface was smoother than the other membranes; and macrovoids were observed. This might have resulted from the combined function of the NaSS and SBMA and caused some special performance. This is discussed in the following sections.

Pure Water Flux Values and Antifouling Properties of the Membranes

The pure water flux, which is an important parameter for UF membranes, was calculated by eq. (2), and the results are shown in Table III. It was apparent that the pure water fluxes for the modified membranes M-1 to M-5 were smaller than that for M-0 and ranged from 528.86 and 120.10 mL m^{-2}·h^{-1}·$mmHg^{-1}$. The reason was that the polymer concentrations for preparing the modified membranes were higher than that for preparing the pristine PES membrane.

BSA solution was then applied to the membranes, and the BSA R values are also shown in Table III. The results show that the R values of the modified membranes were improved compared to that of M-0 membrane. The antifouling properties of the membranes were then investigated with the BSA solution.[40] The antifouling properties could be expressed by the F_{RR} of the PBS solution fluxes before and after BSA solution UF. Figure 4 shows the typical flux curves. We observed that the flux decreased dramatically when the solution changed from PBS to BSA solution because of the fouling caused by the deposition and adsorption of protein molecules onto the membrane surfaces and in the membrane pores.[36] When the adsorption of protein molecules reached a saturation point, a relatively steady flux was obtained at the final stage of the BSA solution UF. After the membranes were washed and PBS was applied to the membranes again, the fluxes of PBS were increased and remained steady after 20 min.

The F_{RR} data are also listed in Table III. We found that the F_{RR} of M-0 was about 70%. After the introduction of the P(SBMA-*co*-NaSS) copolymers into the membranes, the F_{RR} values of all of the modified membranes were increased compared to that of M-0 membrane. The F_{RR}'s of the M-1 to M-4 membranes were above 90%; this was attributed to a decent hydrophilic hydrogel layer caused by the high density of the PSBMA segments on the membrane surfaces. However, the F_{RR} of M-5 (without SBMA) was only about 82.69% for the third cycle. These results indicate that the PSBMA could more efficiently improve the antifouling properties of the membranes compared to NaSS.

Blood Compatibility of the Membranes

Protein Adsorption. Protein adsorption on the material surface is a common phenomenon; it may lead to further negative consequences, such as platelet adhesion, the activation of coagulation pathways, and thrombus formation. The amount of protein adsorbed on the membranes is reported to be of critical importance in the evaluation of the blood compatibility of materials.[41] Thus, in this study, both BSA and BFG were used to evaluate the protein adsorption.

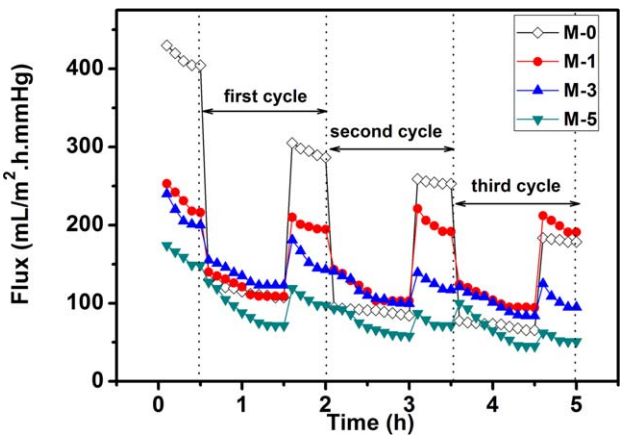

Figure 4. Time-dependent fluxes of the membranes during the process of three cycles of BSA UF at room temperature. Each cycle included UF of the BSA solution (1.0 mg/mL) and then PBS. [Color figure can be viewed in the online issue, which is available at wileyonlinelibrary.com.]

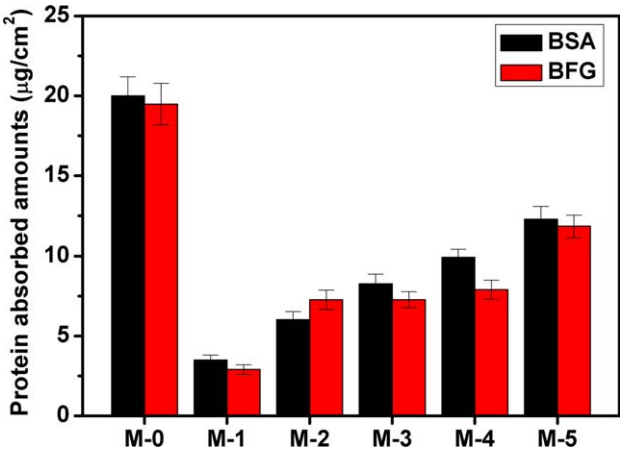

Figure 5. BSA and BFG adsorption onto the pristine and modified PES membrane surfaces. The results are expressed as the means plus or minus the standard deviation ($n = 3$). [Color figure can be viewed in the online issue, which is available at wileyonlinelibrary.com.]

The results of protein adsorption are shown in Figure 5. We found that the modified membranes had lower protein adsorption amounts than the pristine PES membrane. The amount of protein adsorbed on M-1 (only SBMA and without NaSS) was considerably low, only about 3 $\mu g/cm^2$. In addition, the values of BSA and BFG increased with the decrease of SBMA in the copolymerization. Thus, SBMA was more efficient in resisting protein adsorption than NaSS. It has been reported that PSBMA contains both positive and negative charges, which could bind water molecules more strongly and stably via electrostatically induced hydration compared to other hydrophilic materials to achieve surface hydration via hydrogen bonding, and about eight water molecules are tightly bound with one sulfobetaine (SB) unit.[42,43] The protein adsorption amounts were in accordance with the WCA data, as shown in Figure 2, which proved that the adsorption of protein increased with increasing WCA.

Platelet Adhesion. For blood-contacting materials, platelet adhesion is another important parameter in the evaluation of blood compatibility. It is mediated by the integrin on the surface of the platelets, which binds to the adsorbed proteins, especially fibrinogen, and causes platelet activation. The activated platelets then accelerate thrombosis as they promote thrombin formation and platelet aggregation.[41,44] To further study the blood compatibility of these membranes, a platelet adhesion test was carried out, and the shapes of the adhered platelets were observed by SEM.

Figure 6(a) shows the typical SEM pictures of platelets adhering to the membranes. We observed that numerous platelets were aggregated on the pristine PES membrane. Moreover, these platelets spread, flattened, and deformed themselves into irregular shapes, and pseudopodia also stretched out. For the modified membranes, the number of adhered platelets significantly decreased compared to that of the pristine PES membrane, as shown in Figure 6(b). In addition, the platelets retained a rounded morphology with nearly no pseudopodia and deformation. Meanwhile, we found that the amounts of the adhered platelets decreased from M-1 to M-5. This may have been due to the increased BSA adsorption amounts, as shown in Figure 5, and the adsorbed BSA distinctly inhibited platelet adhesion and

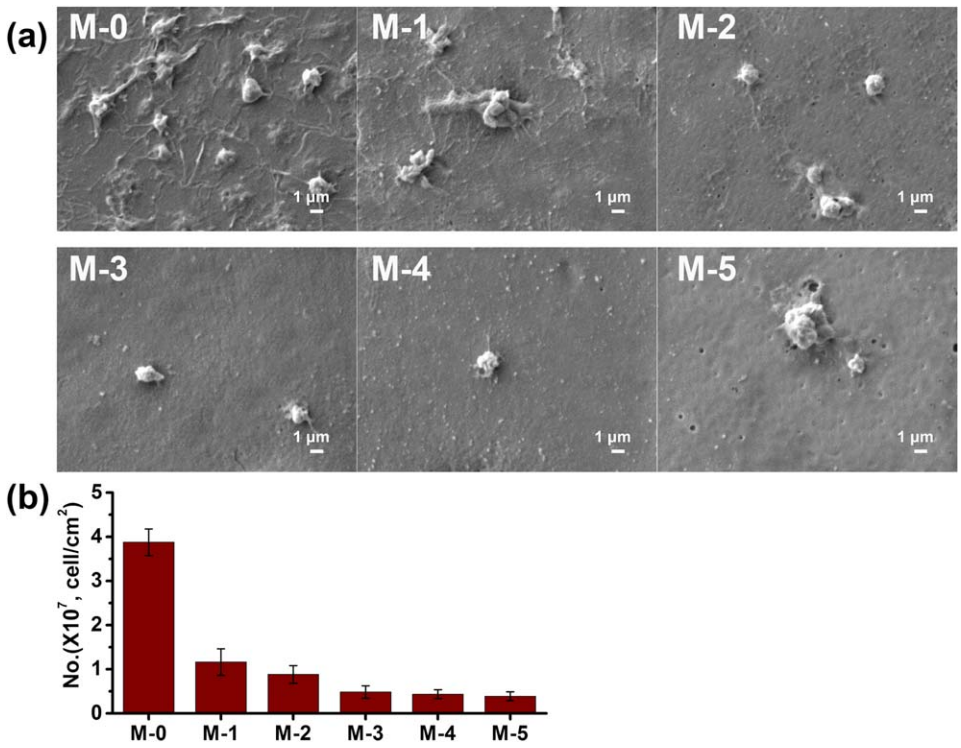

Figure 6. (a) SEM images of the platelets adhering onto the membranes. Magnification = 5000×. (b) Number of adhering platelets onto the membranes from PRP estimated by SEM images. [Color figure can be viewed in the online issue, which is available at wileyonlinelibrary.com.]

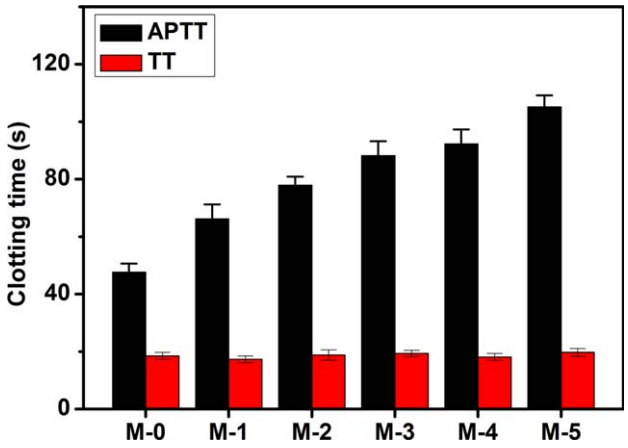

Figure 7. APTTs and TTs for the membranes. The values are expressed as the means plus or minus the standard deviation, $n = 3$. [Color figure can be viewed in the online issue, which is available at wileyonlinelibrary.com.]

aggregation because it is believed that platelet adhesion and spreading will not take place on an albumin-coated surface.[45] Although the BFG adsorbed amounts were also increased, the platelets kept nearly their original morphologies, and pseudopodia were not observed; this resulted from the electrostatic repulsion. The platelet activation was not obvious and could be observed from the SEM image of the platelets. A similar phenomenon was also found in our previous study,[46] in which longer poly(*p*-styrene sulfonate) chain modified membranes showed large BSA and BFG adsorbed amounts and decreased adhered platelets numbers. Thus, it was reasonable that although the adsorbed protein amounts were larger, the adhered platelets numbers were decreased. In addition, the negatively charged pendent sodium sulfonic (—SO_3Na) groups expelled the blood component by electrical repulsion because platelet, red blood cell, plasmatic protein, and other matters in blood show electronegativity. The suppressed platelets adhesion indicated that the blood compatibility for the modified membranes was improved.

Clotting Time. There are three pathways in blood coagulant systems, including the intrinsic pathway, the extrinsic pathway, and the common pathway.[47,48] Recently, APTT and TT tests have been widely used in the evaluation of the *in vitro* antithrombogenicity of biomaterials. The length of APTT reflected the levels of prothrombin, fibrinogen, and blood coagulation factors *V* and *X* in plasma in the endogenous pathway of coagulation. TT test was applied to measure the time taken for a clot to form in the plasma in which an excess of thrombin was added.

Figure 7 shows the clotting times for the PES and modified PES membranes. We found that the APTTs for the modified membranes increased compared with that of the pristine PES membrane. The APTT was prolonged dramatically to about 115 s for M-5, in which the PNaSS content was the highest. The enhancement in the anticoagulant activity indicated that the hydrophilic group (—SO_3Na) might have been available for the binding of coagulation factors.[22] As we know, —SO_3Na groups can bind Ca^{2+}, and this plays an important role in the blood coagulation process. Thus, the clotting time can be prolonged. Meanwhile, in comparison with the results from an earlier study,[17] in which the APTT of the PSf-*g*-PSBMA membranes only slightly increased compared with those of the pristine PSf membrane, the length of APTT reflected the levels of the prothrombin, fibrinogen, and blood coagulation factors *V* and *X* in plasma in the endogenous pathway of coagulation. A TT test was applied to measure the time taken for a clot to form in the plasma, in which an excess of thrombin had been added.[47,49] The TT was unchanged in this test; this indicated that the modified membranes could not influence the process of the transformation between the fibrinogen and the fibrin. However, the APTT was prolonged to 115 s. Thus, the modified membranes had an effect on the endogenous pathway of coagulation and prolonged the clotting time. The anticoagulant properties of the membranes modified with PNaSS were significantly improved in this study.

It was easy to draw the conclusion that the hydrophilic group (—SO_3Na) was an effective group in prolonging the clotting time. The results of APTT and TT testing confirmed the satisfactory blood compatibility of the modified membranes.

CONCLUSIONS

In conclusion, zwitterionic copolymers of P(SBMA-*co*-NaSS) modified PES membranes were successfully prepared by *in situ* crosslinked copolymerization coupled with a liquid–liquid phase-separation technique. On the one hand, the antifouling properties of the SBMA-containing copolymer-modified membranes was tremendously improved, and the F_{RR} was above 90%. On the other hand, the blood compatibility, especially the anticoagulant properties, were significantly improved; the APTT was prolonged to about 115 s. In a word, the PES membranes modified with the P(SBMA-*co*-NaSS) copolymers possessed excellent antifouling properties and blood compatibility and offers potential merit for application in biomedical fields.

ACKNOWLEDGMENTS

This work was financially sponsored by the National Natural Science Foundation of China (contract grant numbers 51173119 and 51225303) and the Program for Changjiang Scholars and Innovative Research Team in University (contract grant number IRT1163). The authors also thank their laboratory members for their generous help and gratefully acknowledge the help of Hui Wang of the Analytical and Testing Center at Sichuan University for SEM.

REFERENCES

1. Mishra, S.; Bajpai, R.; Katare, R.; Bajpai, A. *J. Appl. Polym. Sci.* **2006**, *100*, 2402.
2. Ahmadi, M.; Gorbet, M.; Yeow, J. T. *Blood Purif.* **2013**, *35*, 305.
3. Mao, C.; Qiu, Y. Z.; Sang, H. B.; Mei, H.; Zhu, A. P.; Shen, J.; Lin, S. C. *Adv. Colloid Interface Sci.* **2004**, *110*, 5.
4. Lee, J. H.; Ju, Y. M.; Kim, D. M. *Biomaterials* **2000**, *21*, 683.

5. Zhang, Z.; Zhang, M.; Chen, S.; Horbett, T. A.; Ratner, B. D.; Jiang, S. *Biomaterials* **2008**, *29*, 4285.
6. Zhao, C. S.; Liu, T.; Lu, Z. P.; Cheng, L. P.; Huang, J. *Artif. Organs* **2001**, *25*, 60.
7. Wang, T.; Wang, Y. Q.; Su, Y. L.; Jiang, Z. Y. *J. Membr. Sci.* **2006**, *280*, 343.
8. Zhao, C. S.; Nie, S. Q.; Tang, M.; Sun, S. D. *Prog. Polym. Sci.* **2011**, *36*, 1499.
9. Zhang, Z.; Chen, S. F.; Chang, Y.; Jiang, S. Y. *J. Phys. Chem. B* **2006**, *110*, 10799.
10. Ladd, J.; Zhang, Z.; Chen, S.; Hower, J. C.; Jiang, S. *Biomacromolecules* **2008**, *9*, 1357.
11. Zhu, B.; Xu, X.; Tang, R. *J. Chem. Phys.* **2013**, *139*, 234705.
12. Chen, S.; Li, L.; Zhao, C.; Zheng, J. *Polymer* **2010**, *51*, 5283.
13. Wu, J.; Zhao, C.; Hu, R.; Lin, W.; Wang, Q.; Zhao, J.; Bilinovich, S. M.; Leeper, T. C.; Li, L.; Cheung, H. M. *Acta Biomater.* **2014**, *10*, 751.
14. Schlenoff, J. B. *Langmuir* **2014**.
15. Xiang, T.; Wang, R.; Zhao, W. F.; Zhao, C. S. *Langmuir* **2014**, *30*, 5115.
16. Wu, J.; Lin, W.; Wang, Z.; Chen, S.; Chang, Y. *Langmuir* **2012**, *28*, 7436.
17. Yue, W. W.; Li, H. J.; Xiang, T.; Qin, H.; Sun, S. D.; Zhao, C. S. *J. Membr. Sci.* **2013**, *446*, 79.
18. Gotloib, L.; Shustak, A.; Jaichenko, J. *Nephron* **1989**, *51*, 77.
19. Chang, Y.; Chang, Y.; Higuchi, A.; Shih, Y. J.; Li, P. T.; Chen, W. Y.; Tsai, E. M.; Hsiue, G. H. *Langmuir* **2012**, *28*, 4309.
20. Chang, Y.; Shih, Y. J.; Lai, C. J.; Kung, H. H.; Jiang, S. *Adv. Funct. Mater.* **2013**, *23*, 1100.
21. Mi, L.; Jiang, S. *Angew. Chem.-Int. Ed.* **2014**, *53*, 1746.
22. Ran, F.; Nie, S. Q.; Li, J.; Su, B. H.; Sun, S. D.; Zhao, C. S. *Macromol. Biosci.* **2012**, *12*, 116.
23. Jao, W. C.; Lin, C. H.; Hsieh, J. Y.; Yeh, Y. H.; Liu, C. Y.; Yang, M. C. *Polym. Adv. Technol.* **2010**, *21*, 543.
24. Park, K. D.; Dal Park, H.; Lee, H. J.; Kim, Y. H.; Ooya, T.; Yui, N. *Macromol. Res.* **2004**, *12*, 342.
25. Bowers, V.; Fisher, L.; Francis, G.; Williams, K. *J. Biomed. Mater. Res.* **1989**, *23*, 1453.
26. Park, H. D.; Lee, W. K.; Ooya, T.; Park, K. D.; Kim, Y. H.; Yui, N. *J. Biomed. Mater. Res.* **2002**, *60*, 186.
27. Yu, H. J.; Cao, Y. M.; Kang, G. D.; Liu, J. H.; Li, M.; Yuan, Q. *J. Membr. Sci.* **2009**, *342*, 6.
28. Nam, S. Y.; Lee, Y. M. *J. Membr. Sci.* **1997**, *135*, 161.
29. Steen, M. L.; Jordan, A. C.; Fisher, E. R. *J. Membr. Sci.* **2002**, *204*, 341.
30. Shim, J. K.; Na, H. S.; Lee, Y. M.; Huh, H.; Nho, Y. C. *J. Membr. Sci.* **2001**, *190*, 215.
31. Wavhal, D. S.; Fisher, E. R. *J. Membr. Sci.* **2002**, *209*, 255.
32. Zhang, P. Y.; Xu, Z. L.; Yang, H.; Wei, Y. M.; Wu, W. Z. *Chem. Eng. Sci.* **2013**, *97*, 296.
33. Tao, M.; Liu, F.; Xue, L. *J. Mater. Chem.* **2012**, *22*, 9131.
34. Xiang, T.; Wang, L. R.; Ma, L.; Han, Z. Y.; Wang, R.; Cheng, C.; Xia, Y.; Qin, H.; Zhao, C. S. *Sci. Rep.* **2014**, *4*, 4606.
35. Lowe, A. B.; McCormick, C. L. *Chem. Rev.* **2002**, *102*, 4177.
36. Li, L. L.; Yin, Z. H.; Li, F. L.; Xiang, T.; Chen, Y.; Zhao, C. S. *J. Membr. Sci.* **2010**, *349*, 56.
37. Xiang, T.; Tang, M.; Liu, Y. Q.; Li, H. J.; Li, L.; Cao, W. Y.; Sun, S. D.; Zhao, C. S. *Desalination* **2012**, *295*, 26.
38. Nabe, A.; Staude, E.; Belfort, G. *J. Membr. Sci.* **1997**, *133*, 57.
39. Ran, F.; Nie, S. Q.; Zhao, W. F.; Li, J.; Su, B. H.; Sun, S. D.; Zhao, C. S. *Acta Biomater.* **2011**, *7*, 3370.
40. Shi, Q.; Meng, J. Q.; Xu, R. S.; Du, X. L.; Zhang, Y. F. *J. Membr. Sci.* **2013**, *144*, 50.
41. Tsai, W. B.; Grunkemeier, J. M.; McFarland, C. D.; Horbett, T. A. *J. Biomed. Mater. Res.* **2002**, *60*, 348.
42. Jeon, S. I.; Lee, J. H.; Andrade, J. D.; De Gennes, P. G. *J. Colloid Interface Sci.* **1991**, *142*, 149.
43. Chen, S.; Zheng, J.; Li, L.; Jiang, S. *J. Am. Chem. Soc.* **2005**, *127*, 14473.
44. Grunkemeier, J.; Tsai, W.; McFarland, C.; Horbett, T. *Biomaterials* **2000**, *21*, 2243.
45. Ito, Y.; Sisido, M.; Imanishi, Y. *J. Biomed. Mater. Res.* **1990**, *24*, 227.
46. Xiang, T.; Wang, R.; Qin, H.; Xiang, H.; Su, B. H.; Zhao, C. S. *J. Appl. Polym. Sci.* **2014**.
47. Li, J.; Zhu, B. Q.; Shao, Y. Y.; Liu, X. R.; Yang, X. L.; Yu, Q. *Colloid Surf. B* **2009**, *70*, 15.
48. Lin, W. C.; Liu, T. Y.; Yang, M. C. *Biomaterials* **2004**, *25*, 1947.
49. Xiang, T.; Zhang, L. S.; Wang, R.; Xia, Y.; Su, B. H.; Zhao, C. S. *J. Colloid Interface Sci.* **2014**.